

CrossMark  
click for updatesCite this: *RSC Adv.*, 2017, 7, 403

# Materials with high proton conductivity above 200 °C based on a nanoporous metal–organic framework and non-aqueous ionic media†

Valentina G. Ponomareva,<sup>\*a</sup> Sokhrab B. Aliev,<sup>b</sup> Elena S. Shutova,<sup>a</sup> Denis P. Pishchur,<sup>b</sup> Danil N. Dybtsev<sup>\*bc</sup> and Vladimir P. Fedin<sup>bc</sup>

Fuel cell devices working above 200 °C provide a number of advantages such as low poisoning of the catalyst, high energy output and efficient heat recovery. However, new materials for proton exchange membranes (PEM) must be developed to operate at such conditions. Here we demonstrate that by mixing nanoporous coordination polymer MIL-101 and (benz)imidazolium triflate salts at high pressure with subsequent annealing a hybrid material with superior proton conducting properties approaching 0.1 S cm<sup>−1</sup> at temperatures above 200 °C and in a dry atmosphere could be obtained. The ionic components completely fill the nanopores of the MIL-101 coordination polymer as well as the intercrystallite space, forming a continuous anhydrous proton conducting media. The MIL-101 microcrystalline framework improves the mechanical properties of the material and provides a number of other advantages, such as an increase of the ion conductivity at lower temperatures and a facilitation of the proton transfer by lowering of the activation energy. The present study contains spectroscopic, texture and calorimetric analyses of the reported compounds as well as the investigation of nanoscopic composite effects which affect the phase transition parameters of the ionic components.

Received 20th October 2016  
Accepted 28th November 2016

DOI: 10.1039/c6ra25552c

www.rsc.org/advances

## Introduction

The broad implementation of the energy cycle based on hydrogen fuel is impeded by the absence of certain critical technologies and efficient devices. In particular, the conversion of chemical energy, stored as molecular hydrogen or methanol, into electric power using fuel cells is currently considered the most prominent technological solution. The fuel cells are composed of two electrodes and a proton exchange membrane (PEM), separating the anode and cathode compartments. Current fuel cell devices, however, are very expensive because of polymer membrane material and noble metals, which are used as catalysts for the electrode reactions. Moreover, the prolonged use of fuel cells causes a poisoning of the catalyst by the gas impurities and gradually lowers the device efficiency. The

operation at elevated temperatures not only prevents poisoning but greatly increases the kinetics of the electrochemical reactions,<sup>1</sup> which opens the possibility for the utilization of otherwise less active but a lot cheaper noble-metal-free catalysts. In addition, more efficient heat recovery during the actual device operation is another apparent advantage.<sup>2</sup> As a downside, new proton conducting membrane materials have to be developed because conventional sulfonated organic polymers, such as Nafion, fail to operate above 100 °C or in a dry atmosphere. Acid-doped organic poly-benzimidazole polymers show so far the best proton conducting performance in the temperature range up to 200 °C, but their limited chemical and thermal stability, poor mechanical durability and composite integrity do not allow further temperature increase.<sup>3</sup> Substantial proton conductivity 10<sup>−2</sup> to 10<sup>−1</sup> S cm<sup>−1</sup> at intermediate temperature range 200–250 °C and dry atmosphere for fully inorganic solid electrolytes is achieved when nanoporous or nanostructured materials are modified with acids or acidic salts.<sup>4,5</sup> Most prominent examples involve meso-SiO<sub>2</sub> modified with H<sub>3</sub>PO<sub>4</sub> or heteropolyacids<sup>6,7</sup> as well as CsHSO<sub>4</sub> or CsH<sub>2</sub>PO<sub>4</sub> doped with silica or other oxide ceramics.<sup>8</sup> In such composite systems the highest proton conduction properties result from the enhanced proton mobility and concentration along an extended oxide surface and/or from the facilitation of the supersonic phase transition or nanodispersed state of the corresponding acid salts by the nanoporous ceramic additive. Recently we demonstrated that nanoporous chromium(III) oxoterephthalate metal–

<sup>a</sup>Institute of Solid State Chemistry and Mechanochemistry, Siberian Branch of the Russian Academy of Sciences, 18 Kutateladze st., Novosibirsk, 630128 Russian Federation. E-mail: ponomareva@solid.nsc.ru

<sup>b</sup>Nikolaev Institute of Inorganic Chemistry, Siberian Branch of the Russian Academy of Sciences, 3 Lavrentieva st., Novosibirsk, 630090 Russian Federation. E-mail: dan@niic.nsc.ru

<sup>c</sup>Novosibirsk State University, Department of Natural Sciences, 2 Pirogova st., Novosibirsk, 630090 Russian Federation

† Electronic supplementary information (ESI) available: The details of the instrumental methods (XRD, FT-IR, SEM, TGA, DSC, gas adsorption) and AC impedance measurements, illustrated by the corresponding figures. See DOI: 10.1039/c6ra25552c

organic framework (MOF) MIL-101 (ref. 9) may be utilized as an additive to a solid electrolyte enhancing the conductivity properties, resulting in the proton conductivity for  $(1 - x)\text{CsHSO}_4 - x(\text{MIL-101})$  ( $0.01 \leq x \leq 0.07$ ) composites higher than  $0.01 \text{ S cm}^{-1}$  at  $200^\circ\text{C}$ .<sup>10</sup>

In recent years MOF-based systems have been actively investigating for their proton conduction properties.<sup>11</sup> The overwhelming majority of such compounds are based on aqueous systems, therefore, any substantial conductivity was achieved only for the limited temperature range (below  $100^\circ\text{C}$ ) or in a humid environment. Among the limited number of examples of superionic proton electrolytes ( $\sigma > 10^{-4} \text{ S cm}^{-1}$ ) working above  $120^\circ\text{C}$  in low humidity conditions,<sup>12</sup> the MIL-101 impregnated with aqueous solution of strong inorganic acids features one of the highest conductivity values.<sup>13</sup> In order to extend the temperature stability of such promising systems beyond  $200^\circ\text{C}$  it is necessary to substitute the aqueous media to a low-volatile one. Imidazole and related compounds are known to be great proton conductors. They also have lower volatility, compared with water. In this regard, admixing the MIL-101 to imidazolate salts is a plane and straightforward strategy towards new PEM materials operating at high temperatures and dry atmosphere. The present work demonstrates the successful preparation of solid proton electrolytes composed of porous MIL-101 and imidazolium/benzimidazolium triflates. These hybrid compounds possess remarkable ionic conductivity at temperatures above  $200^\circ\text{C}$  in dry atmosphere, which surpasses the properties of currently investigated materials.

## Experimental section

All chemicals and solvents were at least analytical grade and were used as purchased without additional purification. MIL-101 was synthesized and purified according to the optimized procedure.<sup>13b</sup> The measured BET surface area was  $3580 \text{ m}^2 \text{ g}^{-1}$ . Right before the weight measurements the MIL-101 sample was heated in vacuum at  $180^\circ\text{C}$  for 6 h to remove guest water molecules.

$(\text{C}_3\text{N}_2\text{H}_5)\text{CF}_3\text{SO}_3$  (**1**) was synthesized by admixing the imidazole (0.385 g, 5.67 mmol) with  $\text{CF}_3\text{SO}_3\text{H}$  (0.5 ml, 5.67 mmol) in an argon atmosphere at room temperature. The reaction mixture was crystallized within several minutes. Calculated for  $\text{C}_4\text{H}_5\text{F}_3\text{N}_2\text{O}_3\text{S}$  (%): C, 22.02; H, 2.31; N, 12.84; S, 14.70. Found (%): C, 22.00; H, 2.30; N, 12.62; S, 15.01.

$(\text{C}_7\text{N}_2\text{H}_7)\text{CF}_3\text{SO}_3$  (**2**) was prepared similarly starting from the benzimidazole (0.67 g, 5.67 mmol) and  $\text{CF}_3\text{SO}_3\text{H}$  (0.5 ml, 5.67 mmol). Calculated for  $\text{C}_8\text{H}_7.6\text{F}_3\text{N}_2\text{O}_3.3\text{S}$  (%): C, 35.11; H, 2.80; N, 10.24; S, 11.72. Found (%): C, 35.31; H, 2.67; N, 10.18; S, 12.10.

MIL·10(**1**). **1** (0.068 g, 0.3 mmol) and activated MIL-101 (0.024 g, 0.033 mmol) were thoroughly mixed in a mortar with the following pressing of the mixture at 200 MPa. The obtained pellet was heated for 10 minutes at  $230^\circ\text{C}$ .

MIL·20(**1**) and MIL·20(**2**) were prepared similarly from **1** (0.085 g, 0.39 mmol) and MIL-101 (0.015 g, 0.020 mmol) or from **2** (0.082 g, 0.3 mmol) and MIL-101 (0.012 g, 0.016 mmol), respectively.

## Results and discussion

The imidazolium triflate,  $(\text{C}_3\text{N}_2\text{H}_5)\text{CF}_3\text{SO}_3$  (**1**) and benzimidazolium triflate,  $(\text{C}_7\text{N}_2\text{H}_7)\text{CF}_3\text{SO}_3$  (**2**) were prepared as crystalline compounds by a reaction between the equimolar amounts of the imidazole (benzimidazole) and the triflic acid and characterized by powder X-ray diffraction, IR spectra, chemical and thermal analyses. Both salts are decomposed above  $300^\circ\text{C}$ , thus demonstrating sufficient thermal stability. Some minor weight loss on the TG curve of **2** below  $100^\circ\text{C}$  is attributed to traces of water absorbed from the atmosphere. The DSC measurements showed clear endothermic effects at  $195^\circ\text{C}$  for compound **1** and  $218^\circ\text{C}$  for compound **2**, related to the melting points of these salts.

The MOF-based composite materials were obtained by a mortar mixing of either **1** or **2** with activated MIL-101 ( $[\text{Cr}_3\text{O}(\text{C}_8\text{H}_4\text{O}_4)_3\text{F}]$ ), followed by a pellet pressing at 200 MPa and annealing at  $230^\circ\text{C}$  for 30 min to ensure the space filling not only between the MIL microcrystalline particles but also within its nanopores by the melted triflate salts. Using either 1 : 10 or 1 : 20 MIL-101 to ionic salt ratios we prepared three pellet samples with the following molar compositions: MIL·10(**1**), MIL·20(**1**), MIL·20(**2**). Such formulae correspond to *ca.* 1.5–4 times excess of the salt components compared with the free pore volume of the MIL-101 host framework.<sup>14</sup> The final MIL@salt materials were characterized by powder X-ray diffractions, thermal analyses, gas adsorption measurements, IR spectroscopy and scanning electron microscopy (see ESI†).

The X-ray diffraction data of the MIL@salt composites reveal the superposition of the diffraction peaks from both components, indicating that significant amount of triflate salts comprise the separate crystalline phase gluing the microcrystals of MIL-101. The MIL-101 porous framework mainly remains intact during the pellet fabrication. An absence of the low angle diffraction reflexes could be attributed to some local distortions and mosaicity of the MIL-101 crystal structure upon filling of the pores. Such effects were observed earlier.<sup>13</sup> The SEM images of the composites MIL·10(**1**), MIL·20(**1**) and MIL·10(**2**) also support the preservation of MIL-101 octahedral crystals. The TG data of the samples show no weight loss in the broad temperature range up to  $300^\circ\text{C}$ , where the thermal decomposition begins. The nitrogen adsorption measurements at 77 K suggest that the composite materials possess almost no porosity. The BET specific surface areas, derived from the  $\text{N}_2$  adsorption isotherms at 77 K, were found to be 25, 6.0 and  $16 \text{ m}^2 \text{ g}^{-1}$  for MIL·10(**1**), MIL·20(**1**) and MIL·20(**2**), respectively. These numbers are negligible against those of pristine MIL-101 ( $3580 \text{ m}^2 \text{ g}^{-1}$ ) as well as proposed value for the “MIL + salt” simple mixture of solids (*ca.*  $930\text{--}460 \text{ m}^2 \text{ g}^{-1}$ ), clearly indicating that most of the MIL pores in MIL@salt composites are completely filled with the ionic salt components.

As could be expected for any nanoscaled material, the DSC analysis revealed some downshifts of the phase transition points of nanoscopic salt components compared with the corresponding bulk phases: 1–2.5 K for **1** and 3 K for **2** (Fig. 1). In particular, double peaks for MIL·10(**1**) and MIL·20(**1**) samples



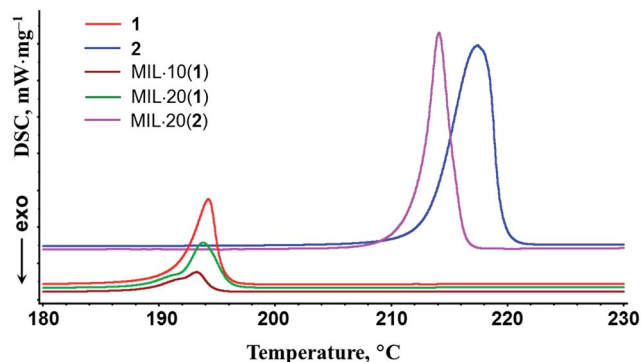


Fig. 1 DSC data of the triflate salts **1**, **2** and the composites MIL·10(**1**), MIL·20(**1**) and MIL·20(**2**). Atmosphere: Ar. Heating rate: 6 deg min<sup>-1</sup>.

on DSC plots indicate the presence of both bulk and MIL-intercalated nanoscopic forms of imidazolium triflate. The DSC plots are completely reversible during multiple consecutive measurements. The pronounced hysteresis between the melting and crystallization temperatures of the (benz)imidazolium triflate salts is also due to a nanocomposite effect and is well consistent with the heterogeneous nature of the samples. The thermodynamic characteristics of imidazolium triflate salts in MIL@salt nanocomposites are also changed markedly. In particular, the melting molar enthalpies of pure ionic salts **1** (6.99 kJ mol<sup>-1</sup>) and **2** (32.2 kJ mol<sup>-1</sup>) are greater than the melting enthalpies adjusted to the actual salt content in the composite samples MIL·10(**1**) (2.93 kJ mol<sup>-1</sup>), MIL·20(**1**) (5.36 kJ mol<sup>-1</sup>) and MIL·20(**2**) (26.3 kJ mol<sup>-1</sup>), indicating a remarkable dispersion and possible partial amorphization of the ionic components.

The AC impedance measurements of the individual salts (**1** and **2**) as well as the composite systems were carried out by a two-probe method using platinum-pressed electrodes in the temperature range from 25 to 240 °C in the atmosphere humidity 0.32 mol% (relative humidity, RH ~ 15% at room temperature). The temperature dependencies of conductivities are presented on Fig. 2. The proton conductivity of **1** steadily increases with temperature whereas the conductivity of **2** decreases at first stage and then increases after heating above 110 °C, which could be attributed to the evaporation of the water impurities from the ionic component **2**. Near the phase transition points of the bulk ionic salts a dramatic (2 to 3 orders of magnitude) increase of the conductivities are observed, followed by relatively flat temperature dependence for the ionic liquids. The complete transition for **1** occurs at 190 °C ( $\sigma = 6.2 \times 10^{-2}$  S cm<sup>-1</sup>) and for **2** at 212 °C ( $\sigma = 3 \times 10^{-2}$  S cm<sup>-1</sup>). A weaker proton conductivity of **2** is explained by a low specific amount of the proton carriers as well as by a greater length for proton hopping in benzimidazolium medium, compared with imidazolium one. The activation energy ( $E_a$ ) of the proton conductivity in the temperature range 100–180 °C could be estimated at 1.0 and 1.28 eV for solid **1** and **2**, respectively, while for the melt state  $E_a = 0.18$  eV for both compounds. The relatively high  $E_a$  values for solid state indicate a mechanism of the proton transfer *via* a formation of intrinsic proton defects or

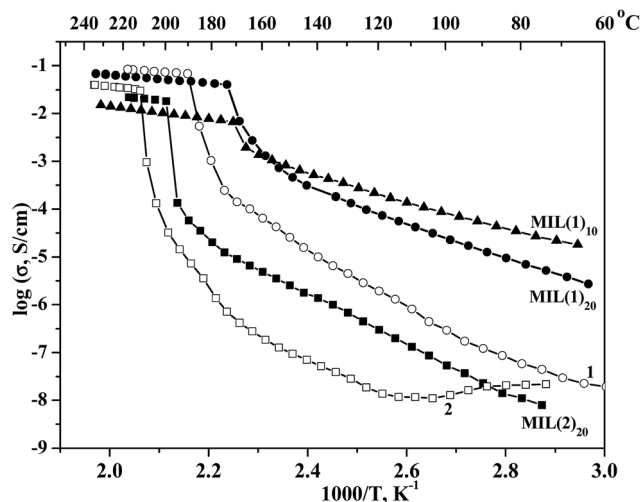


Fig. 2 Temperature dependencies of proton conductivities of triflate salts (open symbols) and composite materials (filled symbols): imidazolium triflate **1** (circles), benzimidazolium triflate **2** (squares), MIL·10(**1**) (triangles), MIL·20(**1**) (circles) and MIL·20(**2**) (squares).

a physical hopping of the protons. Oppositely, low  $E_a = 0.18$  eV is a typical value for the Grotthuss mechanism, involving a transfer of the protons along the H-bond network and simultaneous rotation of the (benz)imidazolium cations, which is consistent with a liquid state of the ionic salts at that conditions.

The impedance measurements of the MIL@salt materials (Fig. 2) indicate the remarkable increase of the ionic salt proton conductivity at lower temperatures upon the addition of MIL-101. The composite effect ranges from 1.5 to 3 orders of magnitudes, depending on the particular mixture composition and the temperature. Such effects are well known and were observed for many composite electrolyte materials, *e.g.* the systems based on acid salts of  $M_nH_m(AO_4)_p$  ( $M = Cs, Rb, K$  and  $NH_4$ ;  $A = S, Se, P$  and  $As$ ,  $n = 1-5$ ,  $m = 1-5$ ,  $p = 1-5$ ) with various heterogeneous matrixes.<sup>6</sup> The proton conductivity of the composite materials with imidazolium salt **1** gradually increase with temperature, starting from  $2 \times 10^{-5}$  S cm<sup>-1</sup> for MIL·10(**1**) and  $3 \times 10^{-6}$  S cm<sup>-1</sup> for MIL·20(**1**) at 60 °C (RH = 0.15) and ending up at  $1.5 \times 10^{-2}$  S cm<sup>-1</sup> for MIL·10(**1**) and  $9 \times 10^{-2}$  S cm<sup>-1</sup> for MIL·20(**1**) at 230 °C (RH ~  $3 \times 10^{-5}$ ). According to the literature data, the last value exceeds by 50% the conductivity of the best electrolyte at such conditions  $H_3PO_4@SiO_2$ .<sup>7</sup> Similarly to the temperature dependence of the proton conductivity of the bulk imidazolium triflate, the data for MIL·10(**1**) and MIL·20(**1**) composites comprise two separate linear ranges with notable phase transition at 165 °C, accompanied by an increase of the conductivity *ca.* 10 times. The stepwise increase of conductivities is consistent with the melting points of the imidazolium triflate salt in the composites MIL·10(**1**) and MIL·20(**1**), independently measured by DSC method. Such phenomenon was observed earlier for MIL-doped  $CsHSO_4$  system as well as for similar solid composite electrolytes and corresponds to the transition of the proton conducting media to high disordered or amorphous state.<sup>8b,8c,10</sup> The  $E_a$  values above 170 °C are as small

as for the liquid **1** (0.18 eV) for both MIL-10(**1**) and MIL-20(**1**), proposing a Grotthuss mechanism of the proton transfer for the composites. Below the melting point the conductivity follows the Arrhenius equation with activation energies  $E_a$  0.53 eV for MIL-10(**1**) and 0.67 eV for MIL-20(**1**), which is noticeably lower than for bulk **1** (1.28 eV). Such dramatic decrease of the activation energy below 170 °C can be explained by a formation of extrinsic defects in the imidazolium triflate phase interacting with the expended MIL-101 surface as well as by a partial amorphization of the encapsulated salt. Such defected structure enables a partial rotation of the imidazolium cations, therefore a mixed Grotthuss — proton hopping mechanism of the ionic conductivity can be speculated at this temperature range. Both high- and low-temperature mechanisms are seemingly maintained over the corresponding linear ranges with no influence from the *e.g.* the atmospheric moisture on the conductivity properties of the samples. It is interesting to note that below the melting temperature the conductivity of MIL-10(**1**) is several times higher than of MIL-20(**1**). This is consistent with the increased ratio of the porous MIL-101 matrix in the nanocomposites and hence with a lower degree of crystallinity of the encapsulated salt, forming conductive pathways for the proton transfer. On the contrary, above 170 °C the conductivity of MIL-20(**1**) with lower MIL content increases five times as a consequence of the percolation effect conductor — insulator. Besides, MIL-20(**1**) contains a higher fraction of the “free” intercrystallite ionic liquid phase of imidazolium triflate than MIL-10(**1**).<sup>14</sup> The conductivity follows the same dependence since the rigid metal–organic framework should slow down the proton transfer inside the MIL-confined imidazolium triflate, compared with that in free state.

The temperature dependence of the conductivity of the composite material with benzimidazolium salt MIL-20(**2**) is also composed of two linear areas with a sharp step at 195 °C, apparently, due to a melting transition of **2**. The activation energies of the proton conductivity, calculated from the Arrhenius equation, are 1.0 and 0.18 eV below and above the melting point. The maximum proton conductivities for MIL-20(**2**) is  $3 \times 10^{-2} \text{ S cm}^{-1}$  at  $T = 230 \text{ °C}$  and relative humidity RH =  $3 \times 10^{-5}$ .

Importantly, the temperature dependence of proton conductivity for the composite materials was successfully reproduced at least two times in full temperature range (both heating and cooling regimes) and no data deviations were observed. We should point out, that the proton conductivity values above 200 °C in dry conditions obtained in this work are among the highest for the studied materials so far. The fuel cell operation at such temperatures greatly increases the chemical reaction kinetics, which should raise the power output of the device. It also reduces the catalyst poisoning, allowing, in principle, the use of less purified fuel or less active noble-metal-free catalysts, both of which reduce the cost of the device and ensure the economic feasibility the corresponding technology.

Although the MIL-101 nanoporous matrix is known to be an ionic insulator, the composite materials show much better performance as the proton electrolytes, compared with the solid salts **1** and **2**. Due to the porous structure and great surface area of MIL-101, high energy of adhesion between the (benz)

imidazolium salts and the metal–organic framework, the conductivity of nanocomposites increases  $10^3$  times at low temperatures. Also, the presence of nanoporous matrix reduces the melting temperatures of the salts (up to 20 K) thus extending the range of the highest proton conductivity of the composite materials. Moreover, the drastic decrease of the activation energies in the studied compounds below the phase transition point suggests an indirect role of the MIL-101 in the proton transfer mechanism by a facilitation of the rotational mobility of the (benz)imidazolium cations, presumably due to weaker intermolecular interactions between the porous framework and the ionic components, compared with those interactions in bulk crystals **1** or **2**. On the other hand, above the melting points, the  $E_a$  values for all compounds are the same (0.18 eV) indicating that the proton transfer in the MIL@salt composite materials is primarily occurs within the ionic liquid component and likely follows the same Grotthuss mechanism. The total filling of the MIL-101 nanopores with the (benz)imidazolium salts establishes the completely anhydrous proton-conducting media of the materials, which maintain their remarkable conductivity properties at a very low atmospheric humidity. It should be also noted, that the rigid structure of MIL-101 acts as an internal structural support of the hybrid material, preserving the pellet shape of the samples and allowing the conductivity measurements at temperatures above the corresponding melting points of the ductile ionic imidazolium components. The stability of the MIL crystalline framework after the multiple measurement cycles was confirmed by impedance data as well as the powder X-ray diffraction. The simple fabrication procedure, high proton conductivity and improved mechanical properties of the composite materials makes them perspective candidates for PEM for fuel cells devices operating at temperatures above 200 °C.

## Conclusions

Simple synthetic method affords new composite materials with superior proton conductivity approaching to  $0.1 \text{ S cm}^{-1}$  at temperatures above 200 °C and dry atmosphere. The imidazolium triflate and benzimidazolium triflate salts completely fill the nanopores of the MIL-101 coordination polymer as well as the intercrystallite space, forming a continuous anhydrous proton conducting media. The crystalline porous framework serves multiple purposes: (a) substantially, up to  $10^3$  times, increases the ion conductivity at lower temperatures due to a nanocomposite effect; (b) reduces the melting points of the impregnated ionic species; (c) facilitates the proton transfer by reducing the activation energy; (d) improves the mechanical properties and maintains the robust shape of the sample at elevated temperatures. The ability to operate at high temperatures makes such hybrid materials perspective for PEM in fuel cells running without costly noble metals.

## Acknowledgements

This work was supported by the grant of the Government of the Russian Federation (PN 14.Z50.31.0006, leading scientist M. Schröder).





## Notes and references

- 1 (a) H. Zhang and P. K. Shen, *Chem. Soc. Rev.*, 2012, **41**, 2382; (b) H. Zhang and P. K. Shen, *Chem. Rev.*, 2012, **112**, 2780.
- 2 (a) S. Bose, T. Kuila, T. X. H. Nguyen, N. H. Kim, K.-t. Lau and J. H. Lee, *Prog. Polym. Sci.*, 2011, **36**, 813; (b) W. H. J. Hogarth, J. C. Diniz da Costa and G. Q. Lu, *J. Power Sources*, 2005, **142**, 223.
- 3 (a) Q. Li, J. O. Jensen, R. F. Savinell and N. J. Bjerrum, *Prog. Polym. Sci.*, 2009, **34**, 449; (b) E. Quartarone and P. Mustarelli, *Energy Environ. Sci.*, 2012, **5**, 6436; (c) S. P. Jiang, *J. Mater. Chem. A*, 2014, **2**, 7637; (d) S. Subianto, *Polym. Int.*, 2014, **63**, 1134; (e) Q. Li, C. Pan, J. O. Jensen, P. Noyé and N. J. Bjerrum, *Chem. Mater.*, 2007, **19**, 350.
- 4 (a) N. F. Uvarov, in *Handbook of Solid State Electrochemistry, Vol. 2: Electrodes, Interfaces and Ceramic Membranes*, ed. V. V. Kharton, Wiley-VCH Verlag, Weinheim, Germany, 2011, pp. 31–71; (b) V. G. Ponomareva and G. V. Lavrova, Fast Proton – Ion Transport Compounds, in *Transworld Research Network*, ed. U. Mioč and M. Davidović, Kerala, India, 2010, pp. 19–42.
- 5 (a) A. Goñi-Urtiaga, D. Presvytes and K. Scott, *Int. J. Hydrogen Energy*, 2012, **37**, 3358; (b) V. Ponomareva and G. Lavrova, *J. Solid State Electrochem.*, 2011, **15**, 213.
- 6 J. Zeng, B. He, K. Lamb, R. De Marco, P. K. Shen and S. P. Jiang, *Chem. Commun.*, 2013, **49**, 4655.
- 7 J. Zeng, Y. Zhou, L. Li and S. P. Jiang, *Phys. Chem. Chem. Phys.*, 2011, **13**, 10249.
- 8 (a) V. G. Ponomareva and E. S. Shutova, *Solid State Ionics*, 2007, **178**, 729; (b) H. Muroyama, K. Kudo, T. Matsui, R. Kikuchi and K. Eguchi, *Solid State Ionics*, 2007, **178**, 1512; (c) V. G. Ponomareva, E. S. Shutova and G. V. Lavrova, *Inorg. Mater.*, 2008, **44**, 1009.
- 9 G. Férey, C. Mellot-Draznieks, C. Serre, F. Millange, J. Dutour, S. Surblé and I. Margiolaki, *Science*, 2005, **309**, 204.
- 10 V. G. Ponomareva, K. A. Kovalenko, A. P. Chupakhin, E. S. Shutova and V. P. Fedin, *Solid State Ionics*, 2012, **225**, 420.
- 11 (a) M. Yoon, K. Suh, S. Natarajan and K. Kim, *Angew. Chem., Int. Ed.*, 2013, **52**, 2688; (b) P. Ramaswamy, N. E. Wong and G. K. H. Shimizu, *Chem. Soc. Rev.*, 2014, **43**, 5913; (c) S. Horike, D. Umeyama and S. Kitagawa, *Acc. Chem. Res.*, 2013, **46**, 2376; (d) T. Yamada, K. Otsubo, R. Makiurac and H. Kitagawa, *Chem. Soc. Rev.*, 2013, **42**, 6655.
- 12 (a) M. Inukai, S. Horike, T. Itakura, R. Shinozaki, N. Ogiwara, D. Umeyama, S. S. Nagarkar, Y. Nishiyama, M. Malon, A. Hayashi, T. Ohhara, R. Kiyanagi and S. Kitagawa, *J. Am. Chem. Soc.*, 2016, **138**, 8505; (b) J. A. Hurd, R. Vaidhyanathan, V. Thangadurai, C. I. Ratcliffe, I. L. Moudrakovski and G. K. H. Shimizu, *Nat. Chem.*, 2009, **1**, 705; (c) D. Umeyama, S. Horike, M. Inukai, Y. Hijikata and S. Kitagawa, *Angew. Chem., Int. Ed.*, 2011, **50**, 11706; (d) S. S. Nagarkar, S. M. Unni, A. Sharma, S. Kurungot and S. K. Ghosh, *Angew. Chem., Int. Ed.*, 2014, **53**, 2638; (e) D. Umeyama, S. Horike, M. Inukai and S. Kitagawa, *J. Am. Chem. Soc.*, 2013, **135**, 11345.
- 13 (a) V. G. Ponomareva, K. A. Kovalenko, A. P. Chupakhin, D. N. Dybtsev, E. S. Shutova and V. P. Fedin, *J. Am. Chem. Soc.*, 2012, **134**, 15640; (b) D. N. Dybtsev, V. G. Ponomareva, S. B. Aliev, A. P. Chupakhin, M. R. Gallyamov, N. K. Moroz, B. A. Kolesov, K. A. Kovalenko, E. S. Shutova and V. P. Fedin, *ACS Appl. Mater. Interfaces*, 2014, **6**, 5161.
- 14 MIL-101 possesses zeotype rigid framework with micropores (diameter  $\approx 11$  Å) and two types of mesopores (diameter  $\approx 29$  and  $34$  Å, respectively, see ref. 9 for the structural details). Taking the estimated molecular volume of the ionic pair (ca.  $300$  Å<sup>3</sup> for **1** and  $400$  Å<sup>3</sup> for **2**) and the guest-accessible pore volume of MIL-101 (80% v/v or ca.  $2000$  Å<sup>3</sup> per MIL-101 formula unit  $[\text{Cr}_3\text{O}(\text{terephthalate})_3(\text{H}_2\text{O})_3\text{F}]$ ), the expected formulae of the host–guest compounds with 100% pore filling should be MIL·7(**1**) and MIL·5(**2**), respectively. In other words, MIL·10(**1**) sample is composed of 75% of guest-filled crystals of MIL-101 and 25% of free **1** (by volume). The volume fraction of such free ionic component in MIL·20(**1**) and MIL·20(**2**) composites is increased to 60% and 70%, respectively.

